IEEE Transactions on Nuclear Science, Vol. NS-26, No. 3, June 1979

PION BEAM DEVELOPMENT FOR THE LAMPF BIOMEDICAL PROJECT*

Michael Paciotti, Howard Amols, James Bradbury, Oliver Rivera†
Kenneth Hogstrom, Alfred Smith††, Hikaru Inoue†††
Daniel Laubacher††††, Scott Sandford†††††

A number of negative pion beam tunes for the LAMPF biomedical channel have been developed for cancer treatments. An extensive catalog of essentially parallel large area beams, up to 300 cm^2, now exists for use in static treatments where the patient is stationary.[1]

Beams are now being optimized specifically for dynamic treatment in which the patient is scanned beneath a beam that is narrow in at least one transverse dimension. We present desired phase-space characteristics of these beams and give beam measurements for some solutions obtained. A new method for field flattening is described that results in more uniform treatment fields than those taken from the relatively flat central regions of very wide pion beams (25-35 cm FWHM).

Common to both static and dynamic treatments is the problem of maintaining good quality control of beams from a secondary channel. A major contributor to therapy beam variation has been change in electron contamination due to change in target geometry and proton beam steering. The electron variation problem is described, and a solution is presented that has been realized as a result of a new target geometry that allows some control of the electron fraction.

Fan Beam Development for Dynamic Treatment

A fan beam is divergent and very broad in the bend plane (XZ) and highly focused in the YZ plane. The patient is scanned along the Y axis, and the resulting sweep over the narrow Y-dose profile produces a flat dose distribution. The depth distribution is varied with the dynamic range shifter[2] as the patient is scanned making possible beam shaping in the YZ plane, a principal advantage of fan-beam treatment.[3]

YZ Plane

The beam at the small waist is Gaussian-shaped with tails of muons from π decay. σ_Y measured in air is held between 1.0 cm and 1.2 cm, the larger size giving higher dose rate and lower convergence in the beam. The rms beam convergence is 120 mrad. The Y-dose profiles measured above and below the waist are nearly unchanged over a 12-cm thickness. The TRANSPORT[4] solutions predict the location of the waist to within a few cm and, it can be positioned[5] as indicated below.

XZ Plane

The X dose profile is to have maximum falloff of 15% over a desired width of 18 cm. A Gaussian-shaped beam with σ_X of 16 cm would satisfy this requirement. Our large beams are usually flatter than Gaussian, and TRANSPORT design σ's of 10-12 cm are usually sufficient. Final beam evaluation is done by dosimetry rather than by particle measurements. The optimum divergence in the XZ plane is dictated by treatment planning. One type of fan beam has 100 mrad rms X divergence and high correlation between angle and position (+1.0 mrad per mm). With this beam an inhomogeneity in the patient[6] receives a small range of angles (25 mrad rms) and can be well-compensated for in this plane by a bolus element at the skin surface, accounting for the average angle of the beam. We also have fan beams with less than half this correlation, in which case the inhomogeneity receives a larger range of angles and the bolus design is more of a compromise. These beams are more suited to parallel beam treatment planning methods.[1]

Fan Beam Field Flattening In The XZ Plane

For the large X-distribution of the fan beam, some of the excess particles in the central region can be removed upstream without affecting the Y-dose profile near the waist. Any upstream location in the channel is suitable if the X-distribution is correlated with the X-distribution at the patient. Rectangular lead blocks are inserted from the +Y and -Y axes at a position 0.6 m upstream in the drift region above the patient where the beam is nearly circular, 16-cm-diameter FWHM. The blocks are 6 cm wide along the X-axis and are inserted far enough to remove some of the core of the X-distribution. The inside edges of the blocks are sloped to match the average angle of the beam, as determined from the particle trajectory tape for the particular fan tune. Final positioning of the blocks is done with dosimetry scans, and results are presented in Fig. 1. The useful width of the resulting beam is increased from 8 cm to 18 cm over the unmodified beam by the selective collimation of 30% of the beam. Also, bolus design is simplified since the pions removed have large Y-angles. The center of the treatment field must be at the Y-waist as the image of the blocks becomes noticeable in the Y-profile measured 8 cm above or below the waist.

Electron Contamination And Its Effect on Therapy Beams

Radiation-Cooled Targets and Electron Production

Electrons arise from conversion of γ rays produced by π° decays. Initial low-power production targets were 2-cm-diameter pyrolytic graphite (ρ = 2.2 g/cm^3) cylinders 8 cm long. The contamination, e^-/π^-, was 0.07 with 20% variation due to the position of the proton beam on the target. Subsequent high-power radiation-cooled targets required larger surface area, being slabs of pyro-graphite 6.5 cm along the proton beam direction, 25 cm tall, and 3 cm wide. A proton beam hitting the center of the 25 cm x 3 cm face provides an average path length for exiting pions of 1.6 cm at our 70° acceptance angle; the path length varies depending on target alignment and proton beam steering. Over a one-year period, e^-/π^- ratios from 0.15 to 0.25 were observed with several targets and steering conditions. Contamination is quoted for a 167 MeV/c beam in an 11.7 m

* Work supported by US PHS Grants CA-16127 and CA-14052 from NCI, and US Department of Energy.

† Los Alamos Scientific Laboratory, Los Alamos, NM 87545.
†† University of New Mexico, Albuquerque, NM 87131
††† Hiroshima University, Hiroshima, Japan
†††† Purdue University, Lafayette, IN 47907
††††† New Mexico Institute of Mining and Technology, Socorro, NM 87801

0018-9499/79/0600-3071$00.75 © 1979 IEEE

channel with the momentum of the first 4.7 m section up to the wedge degrader being 185 MeV/c.

Effect of Be Wedge Degrader on π, μ, and e

The degrader designed to decrease the pion momentum spread introduces a difference in the central momentum of the pion and electron beams of 1.7% at 167 MeV/c as measured by the last bending magnet BM03 used as a magnetic spectrometer[7]; the μ-π difference is 1.4%. Due to multiple scattering and interaction losses, the X-distribution of all particles is biased toward the thin part of the wedge, but in differing amounts. The separation of e^- from π^- in both momentum and position at the wedge leads to spatial separation at the treatment location as most therapy tunes have nonzero spatial dispersion r_{16} and nonzero magnification r_{11} from the wedge to the channel exit. The centroids of the π and e distributions at the treatment location differ by up to 7 cm for different therapy tunes; the μ^--π^- centroid differences are comparable.

Impact Of Off-Center Contamination on Treatment Planning

Although more pions are present per unit total dose on one side of the treatment field than on the other, our present treatment method is based on uniformity of the total dose across the field. The treatment volume is always centered on the channel axis, reducing complication in patient preparation. The total dose profile is also centered on the channel axis; if the profile is not perfectly symmetrical, the 85% falloff points on each side of the beam are centered. To achieve a centered total dose scan in the bend plane, the centroid of the pion beam is displaced, using BM03, from the channel axis on the side opposite the contamination. As electron fraction changes, readjustment of BM03 is required to center the total dose scan. This mis-steering of the pion beam can cause asymmetrical beam loss in the last five quadrupole magnets producing skewed pion distributions.

Water-Cooled Target

A final solution to this problem has awaited the development of the water-cooled pyrolytic graphite production target[8] shown in Fig. 2. The specialized geometry[9] is possible because of the good conductivity properties of pyrographite and the removal of the heat by water cooling.

The vertical position of the target can be varied with respect to the proton beam. The thin vanes provide one tenth the intensity of the thick section of the target. Beam checks are made by scanning the target vertically through the beam and recording the beam rate for each target position. The lower edges of the thin vanes are horizontal, and a scan of this edge gives the proton beam vertical position and width. The edge of the thick part of the target is sloped at 30° from vertical. A vertical scan of this edge through the beam gives the position and size of the proton beam along an axis tilted 30° from the horizontal. The scans indicate Gaussian shapes for the two nearly orthogonal beam profiles with $\sigma \approx 0.35$ cm vertical and $\sigma \approx 0.38$ cm at 30° from the horizontal.

Measurement of Electron Production

Using the time-of-flight method, we measure electrons as a function of the target vertical position. The e^-/π^- fraction is shown in Fig. 3 as a function of the average thickness of pyrocarbon between the proton beam and the entrance to the channel. The full proton beam is intercepted by the thick part of the target for the upper three data points only. For those data points corresponding to the beam partially hitting the thick part of the target, the average carbon thickness for γ-ray conversion is calculated using the proton beam distribution measured with the target scan method.

The relationship between e/π and carbon thickness is approximately linear as expected (neglecting π^- absorption) for π° γ rays converting in the intervening carbon. The slope is 0.09 e^-/π^- at the channel exit per cm of carbon. At zero intervening carbon thickness, e/π is still 0.04; we can account for most of these electrons using the observed conversion rate in carbon. We estimate a contribution of 0.015 e^-/π^- due to conversion in the target box vacuum window and 0.02 e^-/π^- due to internal conversion $\pi^\circ \rightarrow e^+e^-\gamma$. The electron beam has excellent momentum resolution measured at the focal plane indicating that the electrons do come primarily from the target or from target γ's converting in the window. The lowest point on Fig. 3 was obtained with a very low mass target made of a series of 1/16" diameter graphite rods suspended in the beam. The pion rate with this target is only 1% of the full production target. As this data point is consistent with the other data, we conclude that the large mass of carbon in the production target on the side away from the proton beam is not important in electron production.

The presence of the degrader complicates the calculation of e^-/π^- at the target from the measurement at the channel exit. Ignoring the differing interactions between e^- and π^- in the wedge, the ratio at the target is 0.014 e^-/π^- per g/cm^2 of carbon at 70° and 185 MeV/c. Only the pion decay factor (0.30) and a 15% correction for muons under the pion time-of-flight peak have been applied. Measurements will be repeated without the wedge since the correction for it could be 10 to 20 percent.

Operation of the Target

The electron contamination is minimized by placing the sloped carbon edge as close to the center of the proton beam as possible without losing beam on target. The practical limit for this distance is about 0.8 cm representing a little over 2 standard deviations from beam center. We normally operate at 0.85 cm (e^-/π^- = 0.12) and can control the distance to within about 0.1 cm. Checks are made each day before treatment, and adjustment is made on the average once a week.

References

1. Hogstrom, K.R., Smith, A.R., Simon, S.L., Somers, J.W., Lane, R.G., Rosen, I.I., Kelsey, C.A., Kligerman, M.M., von Essen, C.F., Berardo, P.A., and Zink, S.M.: Static pion beam treatment planning of deep-seated tumors using CT scans at LAMPF, to be published in Int. J. of Rad. Oncology, Biology and Physics.

2. Amols, H.I., Liska, D.J., and Halbig, J: Use of a dynamic rangeshifter for modifying the depth dose distributions of negative pions. Med. Phys. 4: 404-407, 1977.

3. Hogstrom, K.R., Smith, A.R., Helland, J.A., Berardo, P.A., Zink, S.M., Paciotti, M.A.: Comparison of static and dynamic pion beam treatment modes at LAMPF; abstract Med. Phys., 5, No. 4, 1978.

4. Brown, K.L., Rothacker, F., Carey, D.C. and Iselin, Ch., SLAC-91 Rev. 1 (1974).

5. Paciotti, M., Bradbury, J., Hutson, R., Knapp, E., and Rivera, O.: Tuning the beam shaping section at the LAMPF Biomedical Channel. IEEE Trans. on Nucl.Sci. NS-24: 1058, 1977.

6. Hogstrom, K.R., Smith, A.R., Somers, J.W., Lane, R.G., Rosen, I.I., Simon, S.L., and Kelsey, C.A.: Measurement of the effect of inhomogeneities and

compensating bolus in clinical pion beams. Submitted to Medical Physics.

7. Paciotti, M.A., Bradbury, J.N., Helland, J.A., Hutson, R.L., Knapp, E.A., Rivera, O.M., Knowles, H.B., and Pfeuffer, G.: Tuning of the first section of the biomedical channel at LAMPF. IEEE Trans. on Nucl. Sci. 22 : 1784, 1975.

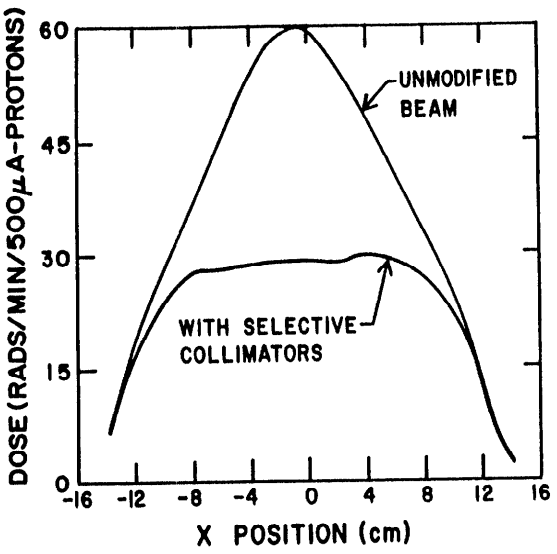

Fig. 1 Fan beam field flattening in the bend plane. Upstream selective collimators remove particles from the peaked central region without affecting the dose profile of the small waist in the other plane. Peak dose rate drops a factor of 2; however, the fraction of beam collimated is only 30%. Doses are measured in a range-shifted beam and are normalized to 500 μA from the accelerator (375 μA on target)

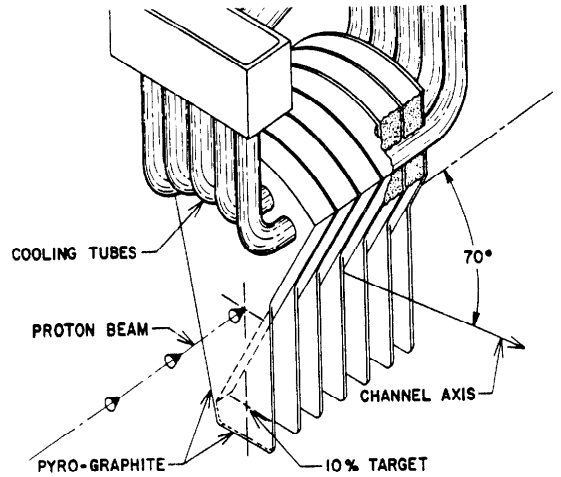

Fig. 2 Pyrolytic graphite (ρ = 2.2 g/cm^3) water-cooled target using copper tubes brazed to graphite.[8] The 768-MeV proton beam is shown intercepted by 6.5 cm of graphite. The vertical position of the assembly is continuously adjustable, allowing scans of the proton beam distributions to be obtained. The thin graphite fins simulate the thick target source but at 10% of the intensity. The pion channel axis is 70° from the proton beam and dips 7.5° below the horizontal.

8. Agnew, L., Grisham, D.L., Lambert, J.E., Thorn, L. L., Holmberg, R. C., Reiswig, R.D., Baldwin, T.S., and Lindquist, L.O.: Graphite targets for use in high intensity proton beams at LAMPF. To be published in the Proc. of the 1979 Particle Accelerator Conference, IEEE Trans. on Nucl. Sci.

9. Dicello, J. and Tschalar, C., first proposed this geometry.

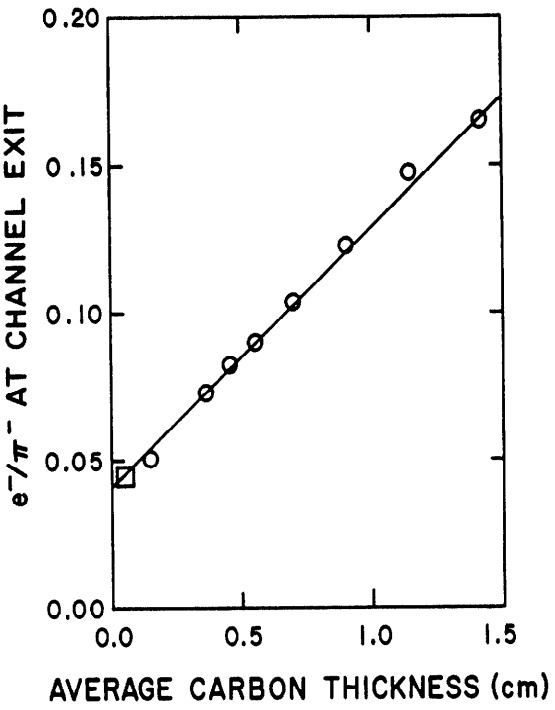

Fig. 3 Electron fraction at 167 MeV/c measured at the exit of the channel as a function of the average graphite (ρ = 2.2 g/cm^3) converter thickness for π° γ rays. Circled data points are measured with the water-cooled target; the variable carbon converter thickness is obtained by vertical adjustment of the sloped carbon face with respect to the proton beam. Converter thickness is averaged over the measured proton beam distribution for data points for which the proton beam partially misses the thick graphite. The contribution of the thin fins is included; the beam lies entirely on the fins for the circled data point at e^-/π^- = 0.05. The single boxed data point is obtained with a very low mass target of thin graphite rods. The e^-/π^- value at zero converter thickness is due to target γ rays converting in the target box window and to e^- from $\pi^\circ \rightarrow e^+e^-\gamma$. The portion of muons that are separable from the pion peak in the time-of-flight spectrum is μ^-/π^- = 0.20, and this value is used to obtain e^-/π^- from the unambiguous measurement of $e^-/(\pi^- + \mu^- + e^-)$. Decays in the last part of the channel are not separable by time-of-flight and have not been corrected for in this figure.